NASA TECHNICAL MEMORANDUM

NASA TM X-71631

NASA TM X-71631

INFLUENCE OF MIXER NOZZLE VELOCITY DECAY CHARACTERISTICS ON CTOL-OTW JET NOISE SHIELDING

by U. von Glahn and D. Groesbeck
Lewis Research Center
Cleveland, Ohio 44135

TECHNICAL PAPER to be presented at
Thirteenth Aerospace Sciences Meeting sponsored
by the American Institute of Aeronautics and Astronautics
Pasadena, California, January 20-22, 1975

INFLUENCE OF MIXER NOZZLE VELOCITY DECAY CHARACTERISTICS ON CTOL-OTW JET NOISE SHIELDING

U. von Glahn† and D. Groesbeck††
V/STOL and Noise Division
Lewis Research Center
National Aeronautics and Space Administration
Cleveland, Ohio

E-8168

Abstract

Jet noise shielding benefits for CTOL engine-over-the-wing configurations were obtained with model-scale multitube and lobed mixer nozzles and various shielding surface geometries. Spectral data were obtained with jet velocities from 585 to 1110 ft/sec. Correlation equations for predicting jet noise shielding benefits with single conical nozzle installations were modified to correlate the mixer nozzle data. The modification included consideration of the number of nozzle elements and the peak axial velocity decay in the flow field adjacent to the shielding surface. The effect of forward velocity on jet noise attenuation by a shielding surface is discussed.

Introduction

In order to reduce jet noise to ground observers, future conventional takeoff and landing (CTOL) aircraft are being considered with engine exhaust nozzles located over the wing (OTW). With such a nozzle-wing configuration, the wing can shield an observer on the ground from significant amounts of jet noise. Jet-noise shielding accomplished by a wing is similar to that observed on the ground by the erection of a barrier between a noise source and an observer. The main differences between the two applications of barrier shielding are the nature and generation mechanisms of the noise source[1] and the close proximity of the noise source to the shielding surface for aircraft compared with ground barrier application.

The acoustic shielding benefits derivable from CTOL wing shielding of jet noise with unattached flow appear to be functions of shielding surface length, nozzle type, nozzle diameter, jet velocity, jet relative velocity, and flap deflection. The effect of the engine location above the wing and the importance of shielding surface length to the acoustic characteristics of CTOL-OTW configurations size has been reported in reference 1 for single conical nozzles. (Other data on jet noise shielding by a wing for the CTOL engine-over-the-wing concept with single nozzles are included in refs. 2 to 4.) The jet noise shielding benefits with a multitube mixer nozzle in a CTOL-OTW orientation are described briefly in reference 5. These data showed that greater jet noise shielding was obtained using a mixer nozzle than with a single conical nozzle for the same total equivalent diameter. A possible reason for this greater shielding is the flow field differences between the mixed flow of a multi-element nozzle and that for a single nozzle of equal flow area. These flow field differences cause an alteration of the noise sources. This alteration is frequently most pronounced in the vicinity of the shielding surface. As a first approximation, the noise sources for multi-element nozzle flows are assumed, herein, to be related to the peak axial velocity decay in the flow field. The pertinent peak velocity is further assumed to be that associated with the downstream edge of the shielding surface.

In the present paper, the flow field and acoustic characteristics of multi-element nozzle CTOL-OTW configurations are first discussed separately. The data include that obtained with small-scale 6- and 8-tube mixer nozzles (nominal equivalent diameter from $1\frac{1}{2}$ to $2\frac{1}{4}$ in.) and an 8-lobe orifice-type mixer nozzle (nominal equivalent diameter, $2\frac{1}{4}$ in.). In addition, data for a large-scale 7-lobe nozzle (nominal equivalent diameter of 15.75 in.) is also included.[6] The acoustic shielding data for multi-element nozzle CTOL-OTW configurations are then correlated with that obtained with single conical nozzle CTOL-OTW configurations.

Acoustic results are presented in terms of spectral data. The data were obtained over a range of nominal jet exhaust velocities from 585 to 1110 ft/sec, depending on the specific nozzle-wing configuration.

Apparatus and Procedure

Facilities

Aerodynamic. For the small-scale models, jet velocity decay measurements were obtained using the static test stand and associated equipment described in reference 7. For the large-scale model, jet velocity decay measurements were obtained at the acoustic test stand as described in reference 6. Nozzle pressure ratios from 1.15 to 2.1 were used. The total temperature of the jet flow was a nominal 520° R.

Acoustic. All the acoustic data herein were obtained using cold-flow (ambient temperature) rigs. The small-scale model data were obtained using the acoustic arenas described in references 1, 5, and 8. The effect of variations in the nozzle-to-shielding surface geometry on the acoustic attenuation were obtained using the courtyard rig described in reference 1. The acoustic data for the large-scale model were obtained using the rig described in reference 6.

The acoustic data herein are presented in terms of sound pressure level spectra in decibels referenced to 2×10^{-5} N/m^2. No corrections are made to the acoustic data for ground reflections. Further details regarding acoustic measurement techniques and procedures are given in references 1 to 8.

Configurations

The multi-element nozzles used in the present study consisted of: a 6-tube mixer nozzle,[5] an 8-tube mixer nozzle,[5] an 8-lobed orifice nozzle,[8] and a 7-lobed mixer nozzle.[6] Sketches of these

†Member AIAA; Chief, Jet Acoustics Branch.

††Aerospace Research Engineer.

nozzles are shown in figures 1 (multitube nozzles) and 2 (lobed nozzles) together with pertinent dimensions.

Two types of surfaces were used to shield the jet noise in the present study: (1) airfoils and (2) simple flat boards. (In ref. 1, it was shown that airfoils and simple boards yield the same amount of jet noise shielding.) The airfoils used are also shown in figures 1 and 2 and are described in the appropriate reference for each nozzle. In addition, simple boards (3/8-in. thick plywood) of 24-inch span and various chordwise lengths were used with the multitube nozzles in order to determine the effect of shielding surface geometry on jet noise attenuation. The various nozzle-shielding surface configurations tested are summarized in figure 3.

Background

Flow Field Considerations

The peak velocity decay for a multi-element nozzle is a function of the mixing characteristics of the jet flow with the ambient (static) or external (forward velocity) flow conditions.[9] Flow fields and/or peak axial velocity decay plots for the present mixer nozzles without the presence of a shielding surface are shown in figures 4 to 7. The flow fields are plotted in terms of constant Mach number lines as a function of radial distance and axial distance measured from and along the nozzle exhaust centerline, respectively. The peak axial velocity decay, also shown in these figures, is plotted in terms of peak Mach number as a function of axial distance measured from the nozzle exhaust plane. Further information regarding these plots is given in references 6, 9, 10, and 11. Also shown at the top portion of figures 4 to 7 is a superimposed schematic sketch of the shielding surface to help relate the shielding surface lengths to the data plots for the specific configuration used. Tick marks on the data plots indicate these shielding lengths. For the 6-tube mixer nozzle data shown in figure 4 the shortest shielding surface, 5.9 inches, provides shielding of jet noise for regions where the individual jet core flows still can be identified. With the longer surfaces the shielding of the jet noise includes regions where the jets are beginning to merge or are actively coalescing into a single large diameter jet. For the other configurations (8-tube and lobed nozzles) the shortest shielding surface generally shields some of the jet flow mixing region as well as the core flow region.

Typical radial profiles of velocity on the tube centerline plane of the 6-tube mixer nozzle are shown in figure 8. At 5.9 inches from the nozzle exhaust plane zero flow exists at the nozzle centerline and the tubes are substantially acting as individual nozzles. With increasing axial distance downstream, the regions along the nozzle centerline begin to fill in until near the end of the longest shielding length used (21.4 in.) the radial velocity profile approaches that for well mixed turbulent flow, both radially and circumferentially. Thus, with increasing shielding length downstream of the core flow region, the board (simulating a wing) shields not only the core flow noise but also increasing amounts of the interaction jet noise sources associated with the jet mixing process. Similar trends exist for the data with the 8-tube mixer nozzle. Both lobed mixer nozzles were tested using shielding surface lengths that covered a significant portion of the merged or coalesced jet flow region. The effect of shielding these various flow regions on jet noise attenuation will be discussed later in terms of peak axial velocity decay characteristics.

Jet Noise Reduction by Surface Shielding

For a CTOL-OTW aircraft, the exhaust jet is located relatively close to the wing surface and is a distributed noise source. The noise obtained at the various frequencies of such an acoustic source is therefore generated at different distances from the surface and at different locations relative to the edge of the barrier (wing or flap trailing edge). An analytical model of the jet noise-source distribution, therefore, would have to include a complex integration to sum up the contributions of all the jet noise sources with their local surface shielding lengths.

The present approach employs empirical correlations of existing data to arrive at a prediction method for the shielding of jet noise by a wing-flap system. The analysis leading to the data correlation is given in terms of the SPL difference between nozzle-plus-shielding-surface and the nozzle-only, $SPL-SPL_N$, or ΔSPL.

A schematic plot of ΔSPL as a function of frequency for a CTOL-OTW configuration is shown in figure 9. Positive ΔSPL values indicate that jet-surface interaction noise sources are dominant over the nozzle-alone jet noise while negative ΔSPL values indicate jet noise shielding by the wing-flap system. Four basic noise regions, denoted by A, B, C, and D are indicated in figure 9. Region A is characterized by noise amplification over that caused by nozzle-alone jet noise and is attributed to jet-surface interaction noise sources. Region B is a transition region into the shielding regime that is a function of the interplay between the regions of interaction noise sources and jet noise shielding. When the interaction jet-surface noise sources are strong (large positive ΔSPL values) the slope of this transition region is steep; whereas when they are weak, the slope of this transition region is shallow and blends rapidly into the jet noise shielding portion of the curve shown. Region C typifies a "barrier" shielding curve. The region C data are used herein to correlate jet noise shielding ΔSPL values. Region D frequently shows a reduced jet noise shielding capability at high frequencies inconsistent with barrier shielding analyses. The exact reasons for reduced jet noise shielding are not understood; however, it is believed that the reduced attenuation is primarily an aeroacoustic interaction (possibly a surface-edge effect) associated with a specific nozzle-wing configuration and reflects the presence of a high frequency noise floor. For jet noise shielding correlation purposes, only the data in region C are directly applicable; the data in region B, however, have been retained in the plots in order to indicate the magnitude of its deviation from the correlation for region C. The data in region D have been deleted in the correlation plots in order to avoid confusing the data trends and correlation.

Application of Single-Nozzle Surface Shielding Results

Single Nozzle Correlation

The acoustic shielding provided by a surface for the noise associated with jet flow from a single conical nozzle[1] was correlated over the same absolute scalar range of variables as those included herein by the following flow and geometry parameters:

$$\Delta SPL \sim \frac{fL}{10^6 U_j} [f_1(D)][f_2(\theta)] = Z \qquad (1)$$

where

$$f_1(D) = \frac{a_o^2}{gD}\left[1 + 4.5\times10^9 \left(\frac{gD}{a_o^2}\right)^2\right] \qquad (2)$$

$$f_2(\theta) = \frac{1}{1 + 0.033\left(\frac{\theta}{180 - \theta}\right)^4} \qquad (3)$$

(All symbols are defined in Nomenclature.) The correlation equation in reference 1 for nozzle-airfoil configuration having zero flap deflection is given by

$$\Delta SPL = 10 \log[1 + 0.6(Z)] \qquad (4)$$

With the flaps deflected, the correlation is given in reference 1 by

$$\Delta SPL = 10 \log[1 + 1.4(Z)^{0.85}] \qquad (5)$$

It should be noted that the acoustic shielding benefits for unattached flow over a surface, such as conical nozzle CTOL-OTW configurations, were substantially independent of nozzle height above the shielding surface.[1]

Also, it was established in reference 1 that for single conical nozzles the effect on jet noise attenuation of whether a simple board or an airfoil was used as the shielding surface was insignificant. Tests were also made herein with the 6- and 8-tube mixer nozzles using both a board and an airfoil and indicated similar results to those in reference 1.

Evaluation of Mixer Nozzles

It is reasonable to expect that when the shielding surface extends only over the jet core region associated with the individual tube or lobe elements of a mixer nozzle, the jet noise shielding can be estimated directly from correlations of acoustic data obtained with a single nozzle of similar size and shape to that of the mixer nozzle elements. In figure 10(a) the ΔSPL obtained with the 6-tube mixer nozzle is plotted as a function of frequency for a shielding surface length of 5.9 inches. The jet core length for a single tube of this mixer nozzle is about 4.7 inches ($X/D \sim 5$). Calculations of the jet spreading angle, indicate that the flows from adjacent jets begin to merge between 4.7 and 6 inches downstream of the exhaust plane. Also shown in the figure are curves for region C representing the calculated ΔSPL values (eq. (4)) for the diameter of an element nozzle, D_x, of 0.93 inch and for the equivalent total nozzle diameter, D_e, of 2.28 inches. Good agreement between the measured and calculated values of ΔSPL is apparent when the element nozzle diameter, D_x, is used in the ΔSPL prediction equation for region C.

When the shielding surface length is sufficient to include the coalescing or mixed jet flow region which has a large effective diameter, it is, perhaps, reasonable to expect that the ΔSPL values for a mixer nozzle could be estimated on the basis of the equivalent nozzle diameter, D_e. The measured ΔSPL obtained with the 6-tube mixer nozzle is plotted as a function of frequency for a shielding length of 21.4 inches in figure 10(b). This shielding length includes much of the coalescing jet flow region as shown in figure 4. Also shown in the figure are curves representing calculated ΔSPL values based on D_x and D_e, respectively. It is apparent that neither calculated curve represents the measured data in region C, although the curve based on D_x is closer to the data.

From the data in figure 10 it would be concluded that the use of D_x in calculating ΔSPL by use of equation (4) for a mixer nozzle is more correct that the use of D_e. However, if a significant change in scale is considered, such as between the 7- and 8-lobed mixer nozzle configurations, a different conclusion emerges. The shielding surfaces cover significant portions of the mixed flow region for both configurations (see figs. 6 and 7). The ΔSPL for the small-scale 8-lobed orifice mixer nozzle (see also appendix A) and the large-scale 7-lobed mixer nozzle configurations are shown in figure 11 as a function of the Z-parameter based on D_x (fig. 11(a)) and D_e (fig. 11(b)). It is apparent that the use of D_e in the Z-parameter correlates the difference in scale whereas the use of D_x fails.

The data, so far, have shown that when substantially only the unmixed core flow of a mixer nozzle is shielded by a surface, the term $f_1(D)$ is based on D_x. For such a case, the single nozzle correlation (eq. (4) for zero flap deflection and eq. (5) for flaps deflected) can be used to predict the ΔSPL for mixer nozzles. However, for cases in which the mixed jet flow is shielded by a surface, $f_1(D)$ is better expressed by using D_e, based on scaling criteria. However, the ΔSPL is not predicted from the single nozzle correlation given by equations (4) or (5) in either case.

Correlation of Mixer Nozzle-Wing Noise Shielding Results

Development of Correlation

The data obtained with the multitube mixer nozzles (see fig. 10) indicated increased jet noise shielding benefits with longer surface lengths even though the Z-parameter already includes a shielding surface length term that correlated the length effect for single conical nozzles. This additional effect on jet noise shielding by increases in shielding surface length is shown in figure 12 in which the ΔSPL is plotted as a function of the product of frequency and length for the 6-tube mixer nozzle configurations. It is apparent that

a systematic variation with surface shielding length occurs when the mixed flow region is shielded, resulting in larger ΔSPL values being obtained with increasing surface shielding lengths. Similar results were obtained with the 8-tube mixer nozzle configurations.

In order to evaluate the relation of shielding length to the flow field in the region between the jet core flow and the coalescing of mixed flow region, the preceding acoustic data obtained with the 6-tube mixer nozzle were used to establish correlation relationships.

The data shown in figure 12 suggest that the noise source alterations associated with the mixed flow region of mixer nozzles influences the jet noise attenuation afforded by a shielding surface. With an increased amount of the mixed flow field being shielded by increased lengths of shielding surface, better acoustic attenuation is provided over a wide range of frequencies. It is postulated that it is possible to characterize the noise source alterations associated with the flow from mixer nozzles by the peak velocity decay in the flow field. Thus, the value of $f_1(D)$ is $f_1(D_x)$ when only the jet core flow is shielded and for mixed flow approaches $f_1(D_e)$ with increasing shielding surface length. It is also postulated that the number of elements of the mixer nozzle contributed to an increase in ΔSPL. On the basis of the present limited data available with mixer-nozzle/wing configurations the following modifications to correlation equations (1) and (2) were developed in order to provide gross ΔSPL predictions for CTOL-OTW configurations using mixer nozzles.

A new parameter, n', which includes the peak velocity decay characteristics in the flow field and gives consideration to the number of nozzle elements, n, has been empirically evolved on the basis of the present data, as follows:

$$n' = 1 + \frac{n - 1}{1 + 0.1\left(\frac{U_j}{U} - 1\right)^{-3}} \qquad (6)$$

The U-term in equation (6) is the peak axial velocity at the location of the trailing edge of the shielding surface. For the present work, the values of U were obtained from the Mach number curves given in figures 4 to 7 at the tick-mark locations for the various shielding surface lengths noted in the figure.

The n'-parameter is used to modify the $f_1(D)$ term (eq. (2)) yielding a new term $f_1(D_e')$, where

$$f_1(D_e') = \frac{a_o^2}{gD_x n'}\left[1 + 4.5\times10^9\left(\frac{gD_x n'}{a_o^2}\right)^2\right] \qquad (7)$$

The Z-parameter (eq. (1)) is modified to include the $f_1(D_e')$ terms as follows:

$$Z' = \frac{10^{-6} fL}{U_j}[f_1(D_e')][f_2(\theta)] \qquad (8)$$

Consequently, equation (4) can now be generalized for single conical and mixer nozzles of the type studied by the following relationship:

$$\Delta SPL = 10 \log[1 + 0.6(Z'n')] \qquad (9)$$

and equation (5) by

$$\Delta SPL = 10 \log[1 + 1.4(Z'n')^{0.85}] \qquad (10)$$

Use of the n'-parameter does not alter the correlation of the single conical nozzle data of reference 1.

The n'-parameter utilizes the jet velocity, U_j, as a baseline velocity term in equation (6). However, it is felt that a better baseline velocity term would be to use the local peak jet velocity when the core jet from one element begins to merge with adjacent core jets. The data used for the present study preclude such an evaluation because the merging point of adjacent jets did not vary sufficiently for the present nozzle configurations. Until such data are available, the use of U_j as the baseline velocity for the n'-parameter is recommended for practical mixer nozzle designs.

Comparison of Measured and Calculated Shielding Data

The measured ΔSPL data are compared with calculated values (solid curves) for the four mixer nozzles used herein in figures 13 to 16. Generally good agreement of the shielding benefits has been achieved with both the board and airfoil surfaces. Because the 6-tube mixer nozzle was used to establish the n'-parameter, the best agreement exists for this nozzle (fig. 13). With the 8-tube mixer nozzle configuration (fig. 14), the data points fall slightly below the predicted values based on equation (9), generally about 1 dB in the region for which the correlation was developed; namely, region C in figure 9.

The 8-lobe orifice nozzle data tend to be somewhat higher than the calculated values based on equation (10) as shown in figure 15. Although the 8-lobe orifice mixer nozzle data appear to indicate a somewhat higher slope in the variation of ΔSPL with the Z'n'-parameter than the multitube data, it is believed that this apparent difference was caused by the flow and acoustic characteristics of the particular orifice-type nozzle used in the tests.

The data for the large-scale 7-lobe nozzle configuration was about 1 dB below the calculated values as shown in figure 16. This small difference may be due, in part, to loss in attenuation caused by the 5^0 angle of the airfoil to the jet flow as discussed in appendix B and shown in figure 2(b).

Effect of Forward Velocity

The data and correlations discussed so far apply to static conditions. The effect of jet relative velocity on the noise attenuation of CTOL-OTW configurations with mixer nozzles, as determined by experiments in a free jet, is discussed in references 1 and 5. In general, the spectra given in references 1 and 5 show that with a constant jet velocity the acoustic attenuation due to the effect of the jet relative velocity is grossly related to the 6-power of the jet relative velocity or

$(U_j - U_o)^6$. This relationship holds for both the spectra and OASPL over a wide range of directivity angles, θ, for CTOL-OTW configurations using mixer nozzles.[5]

In view of the preceding discussion, the following approximate general relation is taken to hold in the flyover plane for the decrease in OASPL in dB due to jet relative velocity effects obtained in a free jet:[12]

$$\Delta OASPL_{RV} = k\langle\theta\rangle \log\left(1 - \frac{U_o}{U_j}\right) \qquad (11)$$

The empirical parameter $k\langle\theta\rangle$ is, at the very least, a function of the directivity angle and amount of noise generated by the interaction of the jet flow with the shielding surface, or added noise. For CTOL-OTW configurations, $k\langle\theta\rangle$ is taken as 60 based on the previously discussed 6-power for the jet relative velocity effects on the SPL spectra. Thus, equation (11) can be expressed as:

$$\Delta OASPL_{RV} = 60 \log\left(1 - \frac{U_o}{U_j}\right) \qquad (12)$$

in dB. Equation (11) applies grossly for directivity angles from 40° to 140°.

In order to obtain preliminary estimates of aircraft motion on the nozzle-wing noise, however, the effect of relative motion of the noise source with respect to the observer must be added to the relative velocity effect measured in a free jet. Because the jet relative velocity effect is given by the 6-power, it is assumed that a quadrupole source is the dominant source affected by forward velocity. As a rough approximation, the convective or Doppler amplification for a quadrupole source can be expressed in dB by

$$\Delta OASPL_D = -60 \log\left[1 - \left(\frac{U_o}{a_o}\right)\cos\theta\right] \qquad (13)$$

and where the Doppler effect on frequency is expressed by

$$f_D = \frac{f}{1 - \left(\frac{U_o}{a_o}\right)\cos\theta} \qquad (14)$$

The two effects of aircraft motion on OASPL can be combined into a single expression to represent the net effect on the nozzle-wing noise. Thus, from equations (12) and (13), the OASPL in dB for a CTOL-OTW configuration is given by

$$OASPL_{FV} = OASPL_\theta - 60 \log\left[1 - \left(\frac{U_o}{a_o}\right)\cos\theta\right] + 60 \log\left[1 - \frac{U_o}{U_j}\right] \qquad (15)$$

In the forward quadrant, the Doppler amplification effect tends to cancel out some of the forward velocity effect. The reverse effect occurs in the rearward quadrant where the convective amplification effect increases the noise attenuation in forward flight.

Examples of the expected effect of aircraft motion on the nozzle-wing noise level based on equation (15) are shown in figure 17. The examples are for jet velocities of 800 and 1600 ft/sec,and a forward velocity of 150 ft/sec. The calculated values are shown in terms of ΔOASPL referenced to static ground OASPL values as a function of directivity angle, θ. Refraction effects on the noise level and directivity are neglected in the example.

With an 800 ft/sec jet velocity (fig. 17(a)), the convective amplification (Doppler) effect would increase the OASPL value obtained in a free jet by about 2.8 dB at $\theta = 40^\circ$, and decrease the OASPL value by a like amount at $\theta = 140^\circ$. At 90° the effect of the convective amplification term is zero. With an increase in jet velocity and a constant forward speed, the convective amplification effect in the forward quadrant (0° to 90°) can more than cancel out the attenuation due to relative velocity measured in a free jet or wind tunnel. An example illustrating this case is shown in figure 17(b). Here, with a jet velocity, U_j, of 1600 ft/sec and a forward velocity, U_o, of 150 ft/sec, the OASPL at a θ of 40° is greater by 0.3 dB with forward velocity than that measured statically. At the same time, the attenuation in the rearward quadrant (90° to 180°) is increased by the convective amplification term over that obtained by the relative velocity effect only.

The preceding illustrative calculations of convective or Doppler amplification effects are considered only indicative of the expected trends and require more research in order to verify the magnitudes of these effects during actual aircraft flight.

Concluding Remarks

The use of mixer nozzles in a CTOL-OTW installation can result in greater jet noise shielding by the wing-flap system than that obtained with a single conical nozzle of equal thrust. When the wing-flap system covers only the unmerged flow region from the individual elements of a mixer nozzle, the jet noise shielding benefits, in terms of ΔSPL, can be predicted from the single conical nozzle correlation equations of reference 1. In these correlation equations, the diameter term is that of an element nozzle of the mixer nozzle. However, when the wing-flap system includes coverage of the mixed flow region of a mixer nozzle, an additional parameter consisting of the number of elements comprising the mixer nozzle and the jet velocity at the end of the shielding surface must be included. The latter parameter also includes consideration of the peak axial velocity decay for the mixer nozzle.

Appendix A

Acoustic Data for CTOL-OTW Configuration Using 8-Lobed Orifice Mixer Nozzle

As part of the acoustic program reported in reference 8, SPL data (unpublished) were also obtained with the 8-lobe orifice nozzle without using a deflector to attach the flow to the airfoil surface. These unpublished data are representative

of a CTOL-OTW configuration with unattached flow and are shown in figure 18 for a directivity angle of 100°. The data are presented in terms of ΔSPL as a function of frequency normalized for various jet velocities, f/U_j, and for total flap deflection angles of 20° and 60°. The data for a jet velocity of 744 ft/sec are used in the present paper as an example for comparison with an empirical correlation equation for predicting the shielding benefits when a lobed mixer nozzle is used.

Appendix B

Effect of Shielding Surface Angularity on Jet Noise Shielding

The large-scale, 7-lobe mixer nozzle data (fig. 11) was obtained originally as part of the engine under-the-wing externally blown flap study reported in reference 6. For that study the nozzle was canted 5° toward the airfoil chordline and the data reported were for the region under the wing. Microphones, however, were also placed above the wing and these constitute the large-scale model acoustic data source for the present OTW report. Thus, for the OTW orientation, the airfoil was angled 5° into the jet flow. In order to determine the effect of nozzle-airfoil angularity on the acoustic shielding, data were obtained using a 2.14-inch diameter nozzle with a board acting as the shielding surface. Acoustic data obtained with this nozzle and with the board angled away from the jet axis (up to 15°) were reported previously in reference 1. For the present work, the board (L = 10.4 in.) was angled 5° and 10° into the jet flow. The nozzle was located 1.75 inches above the board surface. The results of these board angles on the jet noise shielding are shown in figure 19 for a jet velocity of 672 ft/sec. At a 5° board angle into the jet flow, the ΔSPL's attained were substantially the same values as at a 0° board angle. Only the initiation of shielding benefits was affected by the 5° angularity. This latter result was obtained because the low frequency noise was increased and extended to higher frequencies compared with that at the 0° board angle. At the 10° board angle, the ΔSPL were substantially reduced at all frequencies at which jet noise shielding occurred. On the basis of these results, it is concluded that the ΔSPL values measured for the present 7-lobed mixer nozzle-airfoil configuration could only have been slightly affected by the 5° angularity of the airfoil relative to the nozzle jet flow.

The correlation of the jet noise shielding benefits for CTOL-OTW configurations with multi-element mixer nozzles is based on a limited range of 6 to 8 nozzle elements. Further work using nozzles with fewer and greater numbers of nozzle elements and with various spacings between the elements should be conducted in order to determine the validity of the correlation presented herein over a wide range of mixer nozzle geometries.

Nomenclature

a_o ambient speed of sound

D nozzle diameter

D_e equivalent total nozzle diameter

D_e' effective nozzle diameter

D_x equivalent element nozzle diameter

f 1/3 octave band spectrum frequency

f_1, f_2 functional notation

g constant, 32.2 ft/sec^2

h nozzle (or nozzle element) height above surface at exhaust plane

$k(\theta)$ empirical parameter characterizing directivity angle and interaction noise effects

L shielding surface length downstream of nozzle exhaust plane

L_f shielding surface length upstream of nozzle exhaust plane

M local jet Mach number

M_j jet Mach number at nozzle exhaust plane

M_p peak local jet Mach number

n number of elements in mixer nozzle

n' source alteration parameter

OASPL overall sound pressure level, dB, re 2×10^{-5} N/m^2

SPL sound pressure level of nozzle-surface configuration, dB, re 2×10^{-5} N/m^2

ΔSPL SPL - SPL_N, dB

SPL_N sound pressure level of nozzle only, dB, re 2×10^{-5} N/m^2

U peak local axial velocity

U_j jet velocity at nozzle exhaust plane

U_o forward velocity

X axial distance downstream of nozzle exhaust plane

Z,Z' jet noise shielding correlation parameters

α surface deflection angle

θ directivity angle measured from inlet

Subscripts:

D Doppler

FV forward velocity

RV relative velocity

θ angular location notation for forward velocity equations

References

1. von Glahn, U., Groesbeck, D. and Reshotko, M., "Geometry Considerations for Jet Noise Shielding with CTOL Engine-Over-the-Wing Concept," AIAA Paper 74-568, Palo Alto, Calif., June 17-19, 1974.

2. Reshotko, M., Olsen, W. A., and Dorsch, R. G., "Preliminary Noise Tests of the Engine-Over-the-Wing Concept. 1: 30 Deg - 60 Deg Flap Position," TM X-68032, 1972, NASA.

3. Reshotko, M., Olsen, W. A., and Dorsch, R. G., "Preliminary Noise Tests of the Engine-Over-the-Wing Concept. 2: 10 Deg - 20 Deg Flap Position," TM X-68104, 1972, NASA.

4. Reshotko, M., Goodykoontz, J. H., and Dorsch, R. G., "Engine-Over-the-Wing Noise Research," AIAA Paper 73-631, Palm Springs, Calif., July 1973.

5. von Glahn, U., Goodykoontz, J. and Wagner, J., "Nozzle Geometry and Forward Velocity Effects on Noise for CTOL Engine-Over-the-Wing Concept," presented at the Eighty-Sixth Meeting of the Acoustical Society of America, Los Angeles, Calif., Oct. 30 - Nov. 2, 1973. TM X 71453, 1973, NASA.

6. Goodykoontz, J. H., Wagner, J. M. and Sargent, N. B., "Noise Measurements for Various Configurations of a Model of a Mixer Nozzle - Externally Blown Flap System," TM X-2776, 1973, NASA.

7. McKinzie, D. J., Jr., and Burns, R. J., "Externally Blown Flap Trailing Edge Noise Reduction by Slot Blowing: A Preliminary Study," TM X-68172, 1973, NASA.

8. Olsen, W. A., and Friedman, R., "Noise Tests of a Model Engine-Over-the-Wing STOL Configuration Using a Multijet Nozzle with Deflector," TM X-2871, 1973, NASA.

9. von Glahn, U. H., Groesbeck, D. E. and Huff, R. G., "Peak Axial-Velocity Decay with Single- and Multi-Element Nozzles," AIAA Paper 72-48, San Diego, Calif., Jan. 1972.

10. Goodykoontz, J. H., Olsen, W. A. and Dorsch, R. G., "Small-Scale Tests of the Mixer Nozzle Concept for Reducing Blown-Flap Noise," TM X-2638, 1972, NASA.

11. von Glahn, U., Groesbeck, D. and Goodykoontz, J., "Velocity Decay and Acoustic Characteristics of Various Nozzle Geometries with Forward Velocity," AIAA Paper 73-629, Palm Springs, Calif., July 1973.

12. Dorsch, R. G., "Externally Blown Flap Noise Research," SAE Paper 740468, Dallas, Tex., Apr.-May 1974.

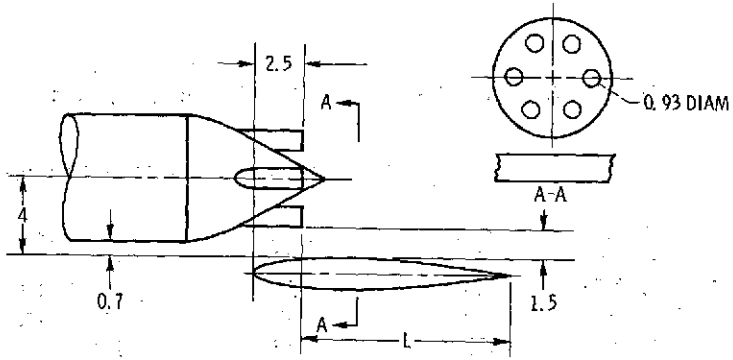

(a) 6-TUBE MIXER NOZZLE.

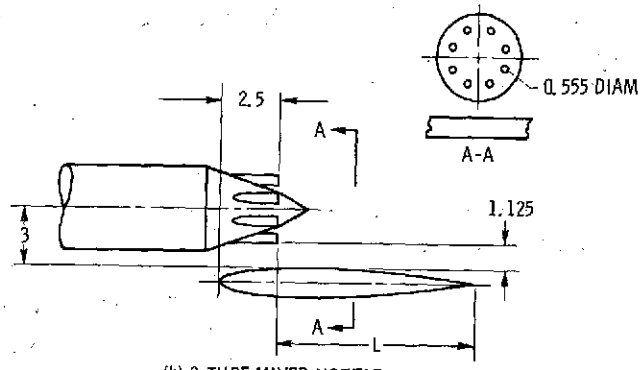

(b) 8-TUBE MIXER NOZZLE.

Figure 1. - Multitube mixer nozzle CTOL-OTW configurations. All dimensions in inches. Reference 5.

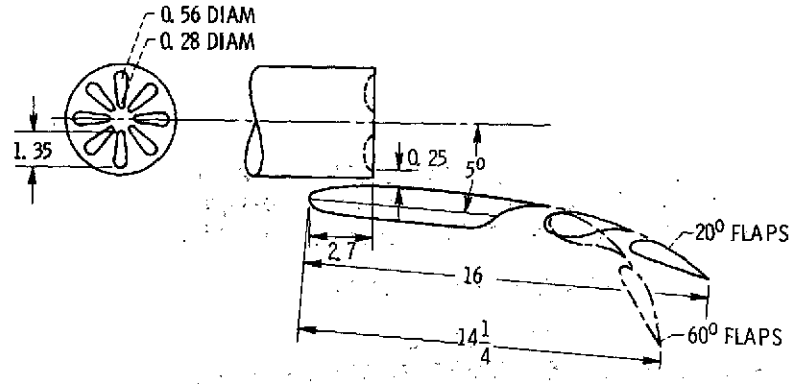

(a) 8-LOBED ORIFICE NOZZLE, REF. 8.

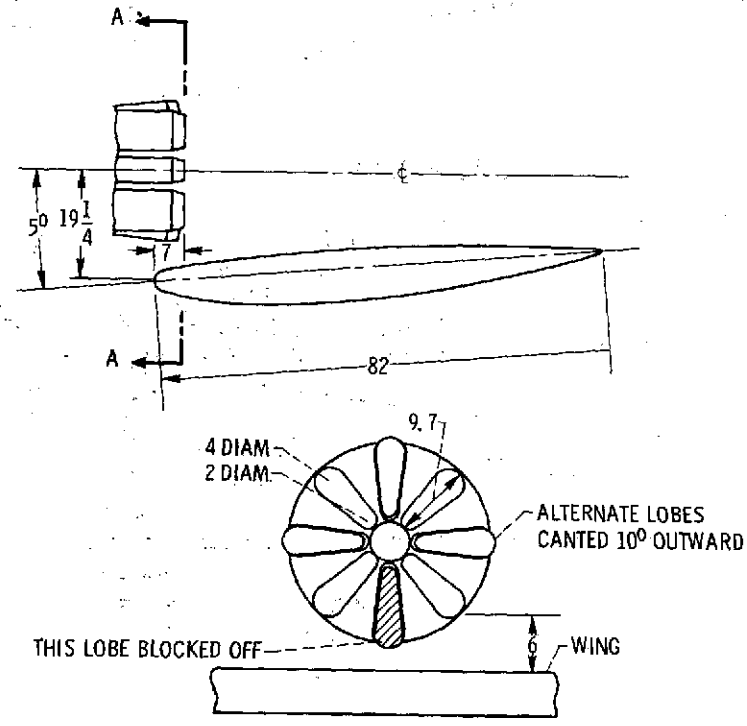

VIEW A-A

(b) 7-LOBE NOZZLE, REF. 6.

Figure 2. - Sketch of mixer nozzles with wing. All dimensions in inches.

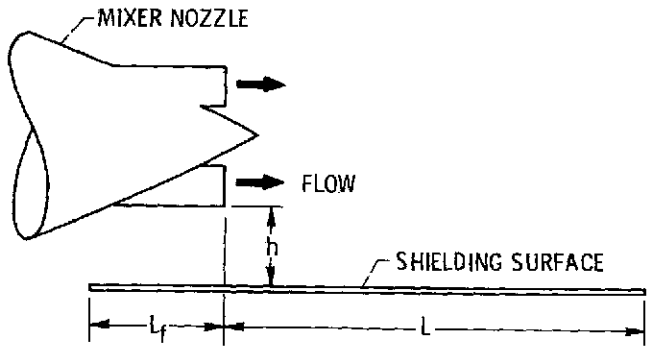

NOZZLE	L_f, IN.	L, IN.	h, IN.	SHIELDING SURFACE
6-TUBE	2.6	5.9, 7, 8, 9, 10.4, 21.4	1.5, 1.75	BOARD
	2.6	10.4	1.5	AIRFOIL
8-TUBE	2.6	5.9, 8.1, 10.4	1.125	BOARD
	2.6	10.4	1.125	AIRFOIL
7-LOBE	7	75	6	AIRFOIL
8-LOBE	2.7	13.3	0.5	AIRFOIL, 20^0 FLAPS
	2.7	11.6	0.5	AIRFOIL, 60^0 FLAPS
CIRCULAR	2.6	10.4	1.75	[a]BOARD

[a]BOARD DEFLECTED INTO JET FLOW, 5^0 AND 10^0.

Figure 3. - Summary of shielding surface configurations. All dimensions in inches.

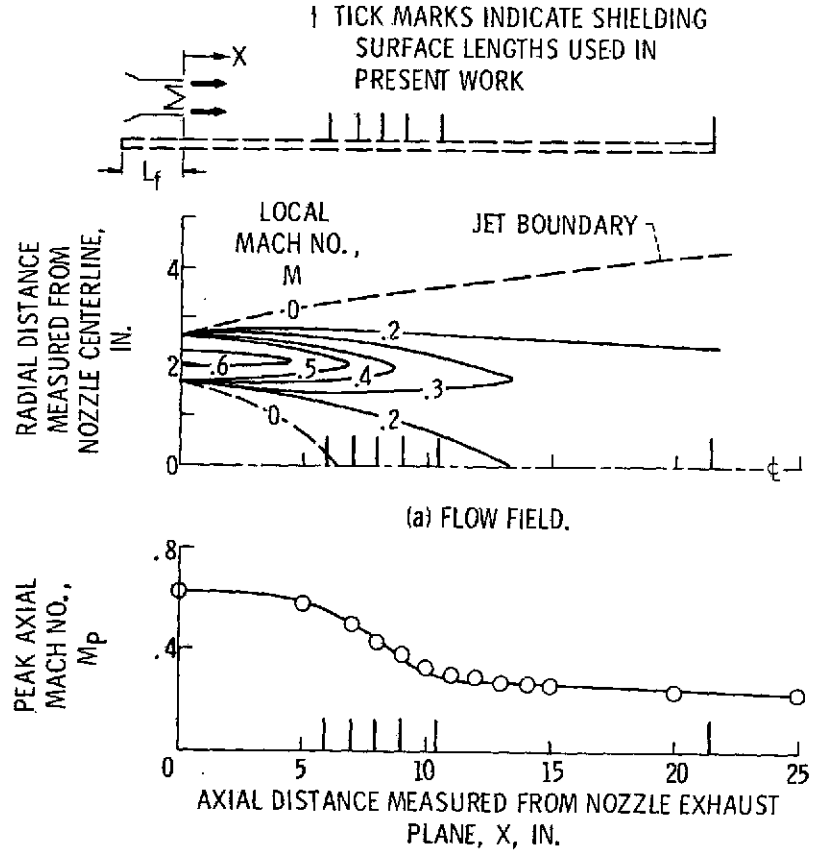

Figure 4. - Flow field and peak axial velocity decay characteristics for 6-tube mixer nozzle only. M_j, 0.62; L_f, 2.6 in.; data from ref. 9.

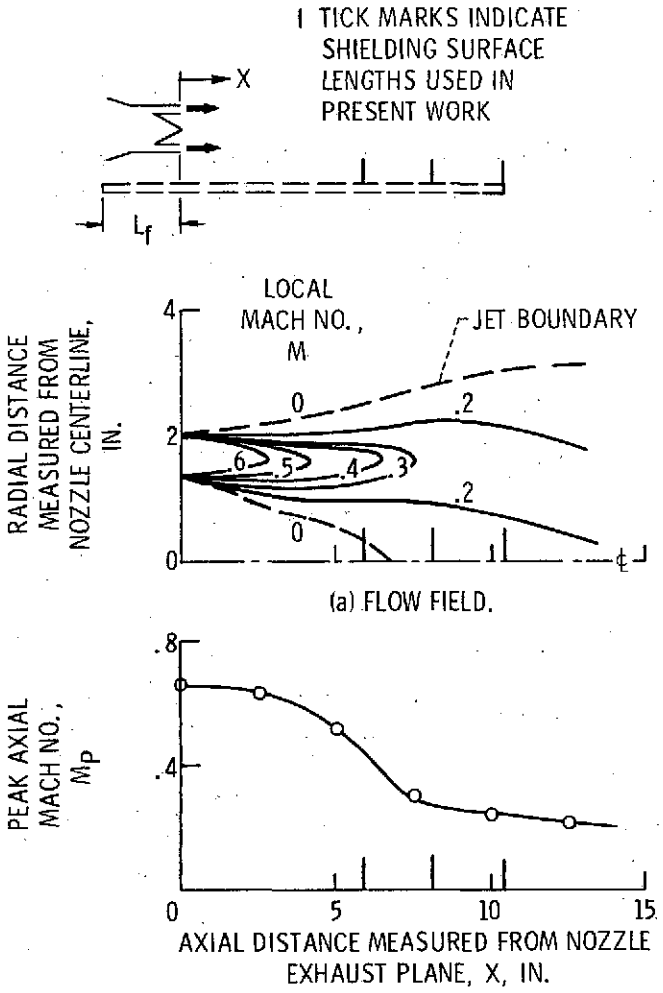

Figure 5. - Flow field and peak axial velocity decay characteristics for 8-tube mixer nozzle only. M_j, 0.64; L_f, 2.6 in.; data from ref. 9.

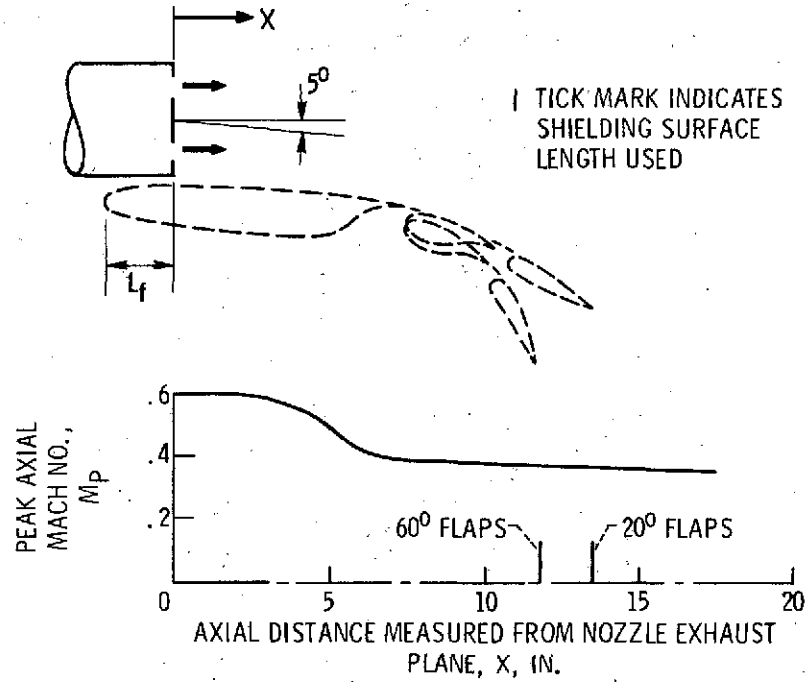

Figure 6. - Peak axial velocity decay characteristics for 8-lobed orifice mixer nozzle only extrapolated from ref. 10. M_j, 0.6; L_f, 2.7 in.

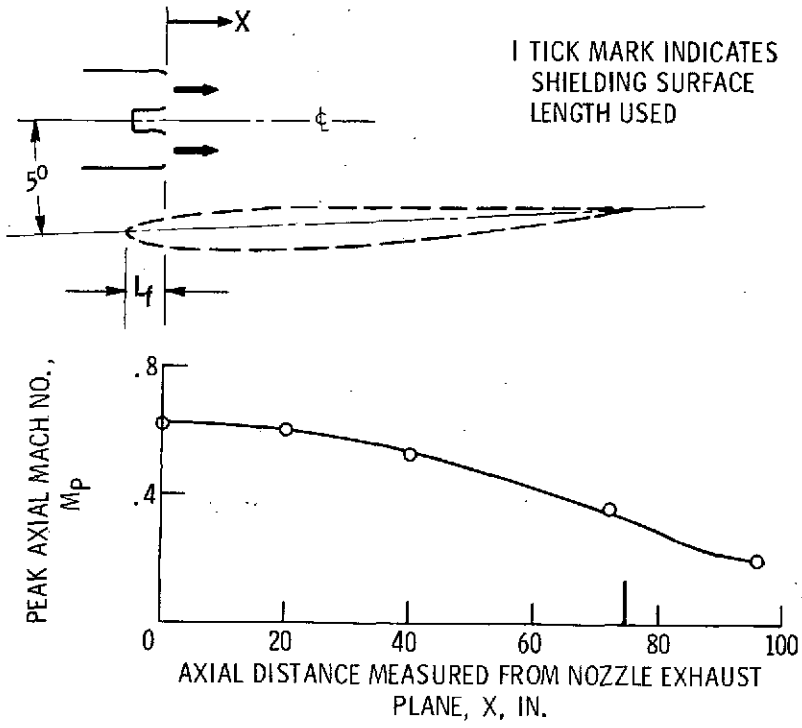

Figure 7. - Peak axial velocity decay characteristics for 7-lobed mixer nozzle only. M_j, 0.62; L_f, 7 in.; data taken from ref. 6.

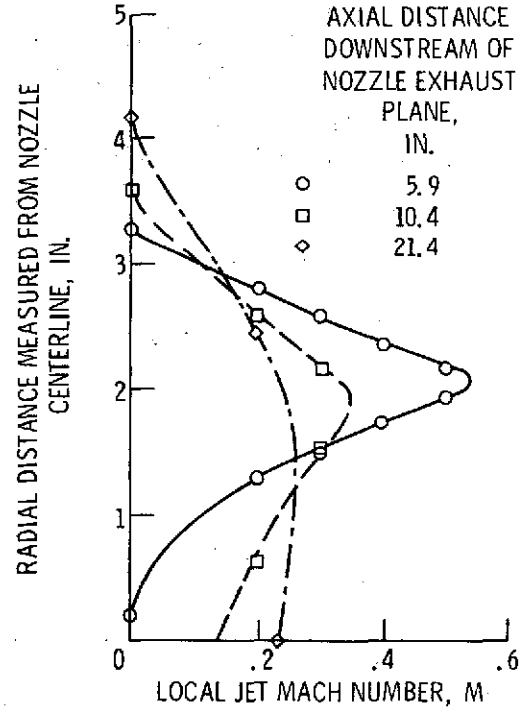

Figure 8. - Radial profiles of velocity for several axial locations downstream of 6-tube mixer nozzle. M_j, 0.62; tube centerline plane.

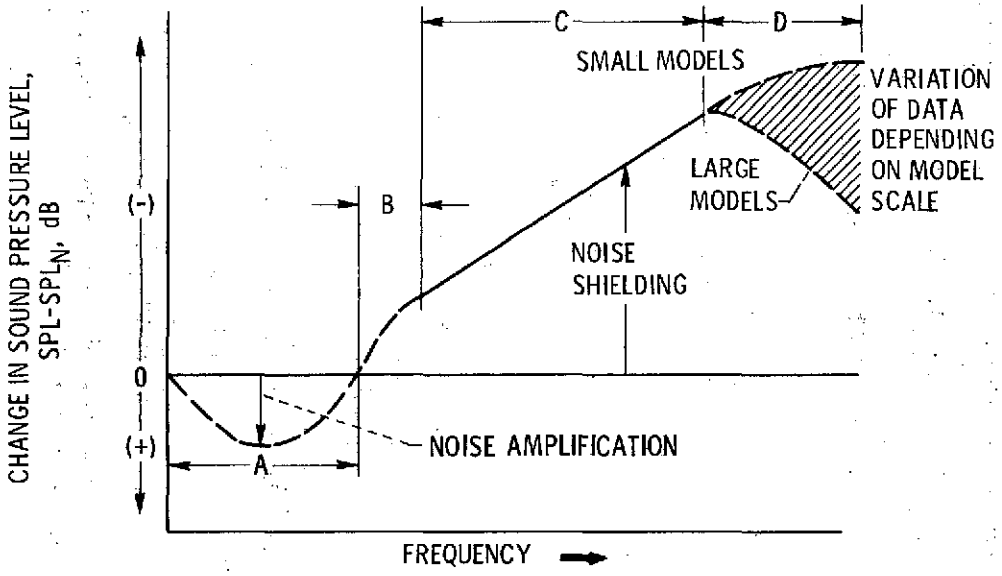

Figure 9. - Schematic representation of change in sound pressure level of jet noise due to a shielding surface.

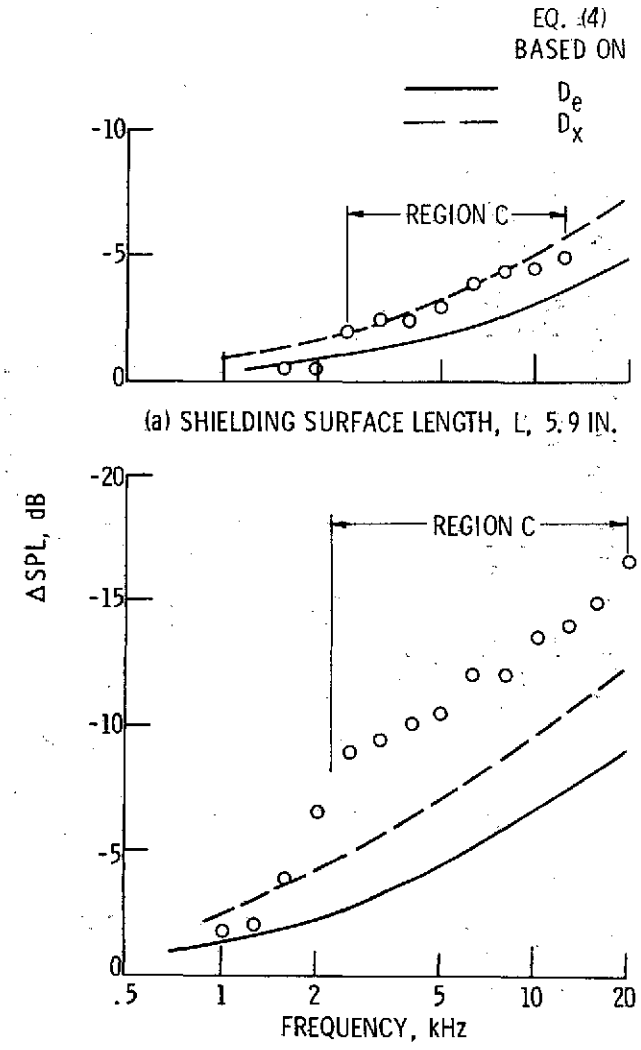

Figure 10. - Comparison of measured ΔSPL for 6-tube mixer nozzle with calculated ΔSPL for single conical nozzle. Jet velocity, 665 ft/sec; directivity angle, 90°.

	L/D_x	D_x, FT	NOZZLE	θ, DEG	u_j, FT/SEC	L/D_e	D_e, FT
○	12.5	0.5	7-LOBE	90	670	4.76	1.31
□	12.5	.5	7-LOBE	90	938	4.76	1.31
◇	16.1	.0775	8-LOBE	100	744	6.33	0.198

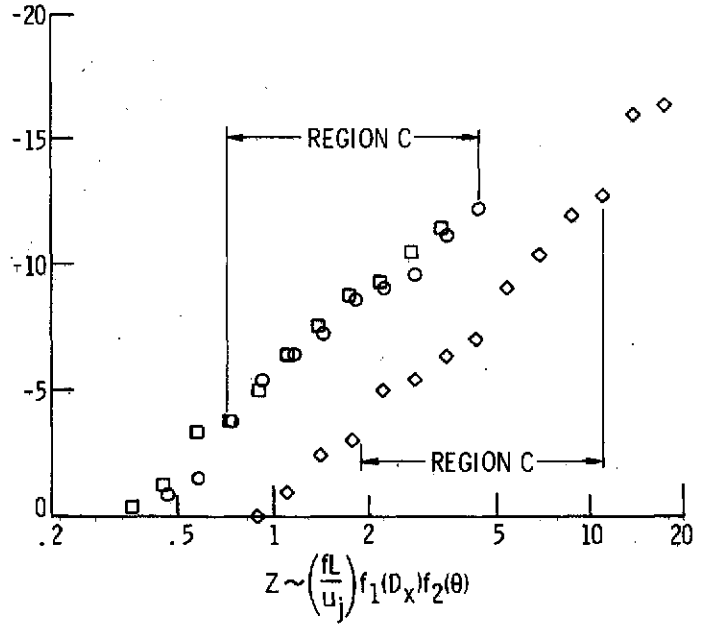

(a) Z-PARAMETER BASED ON D_x.

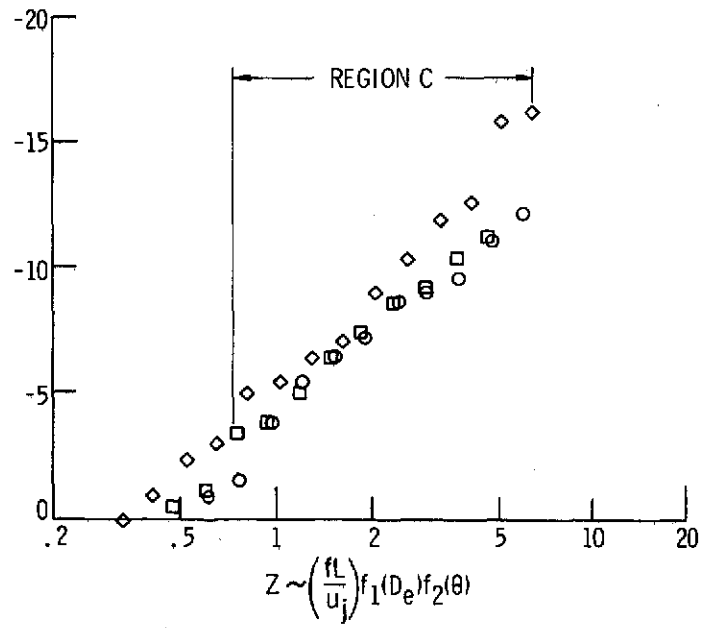

(b) Z-PARAMETER BASED ON D_e.

Figure 11. - Correlation of ΔSPL in terms of Z-parameter from ref. 1 for lobed mixer nozzles.

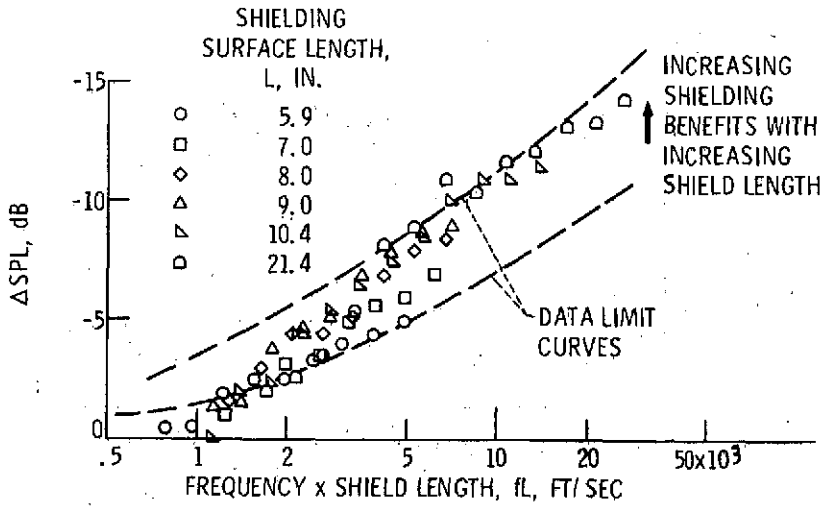

Figure 12. - Effect of shield length on jet noise shielding benefits with a 6-tube mixer nozzle. Jet velocity, 665 ft/sec; directivity angle, 90°.

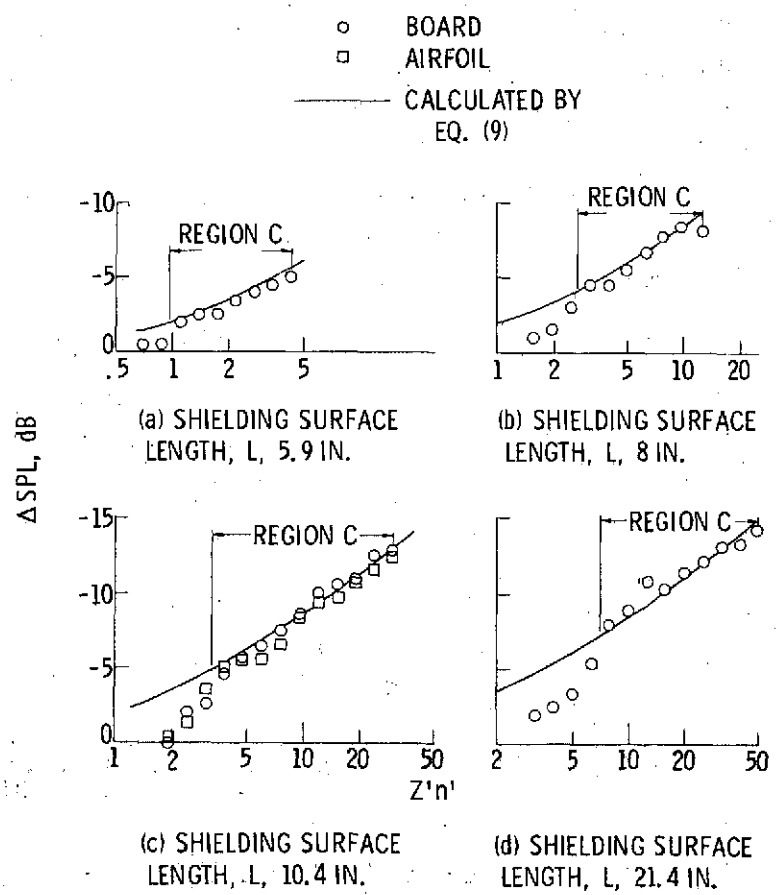

Figure 13. - Comparison of measured jet noise shielding benefits with calculated values for various shielding surface lengths. 6-Tube mixer nozzle; jet velocity, 665 ft/sec; directivity angle, 90°.

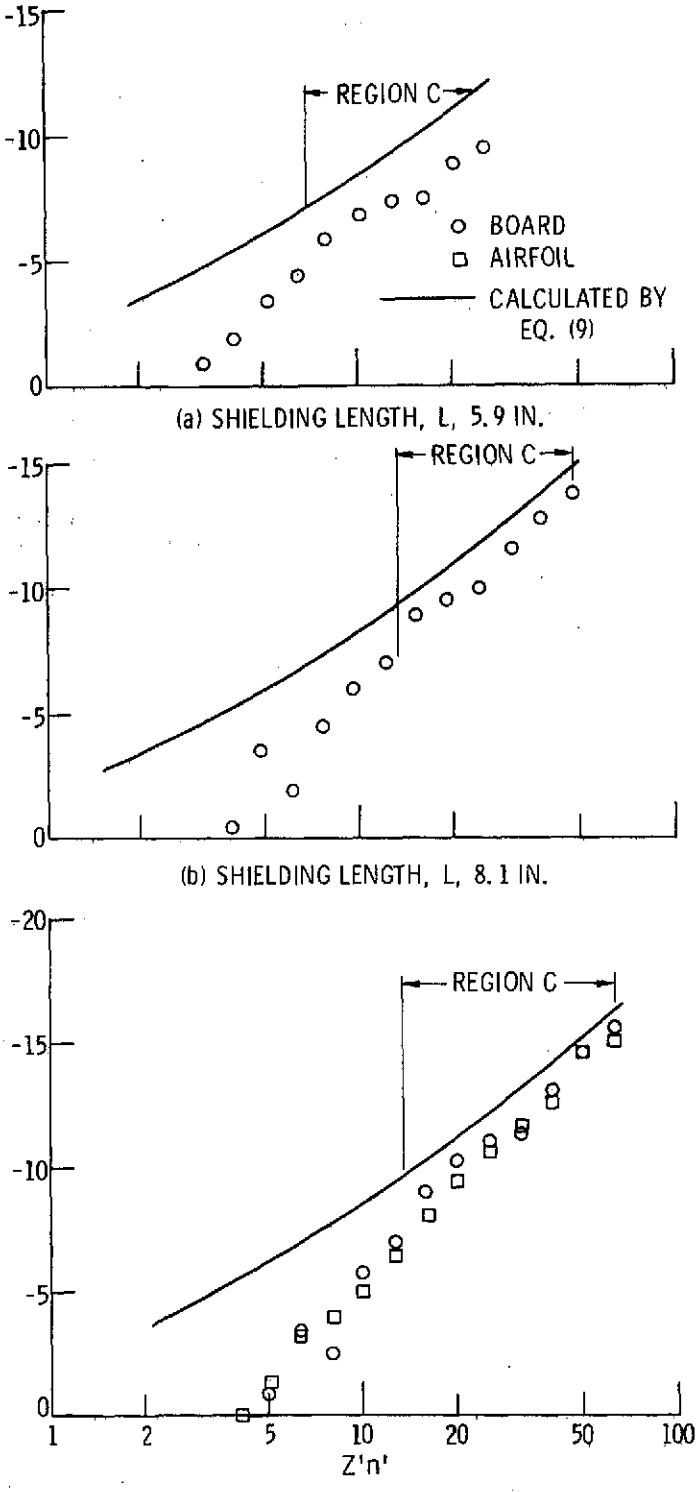

(a) SHIELDING LENGTH, L, 5.9 IN.

(b) SHIELDING LENGTH, L, 8.1 IN.

(c) SHIELDING LENGTH, L, 10.4 IN.

Figure 14. - Comparison of measured jet noise shielding benefits with calculated values for various shielding surface lengths. 8-Tube mixer nozzle; jet velocity, 656 ft/sec; directivity angle, 90°.

E-8168

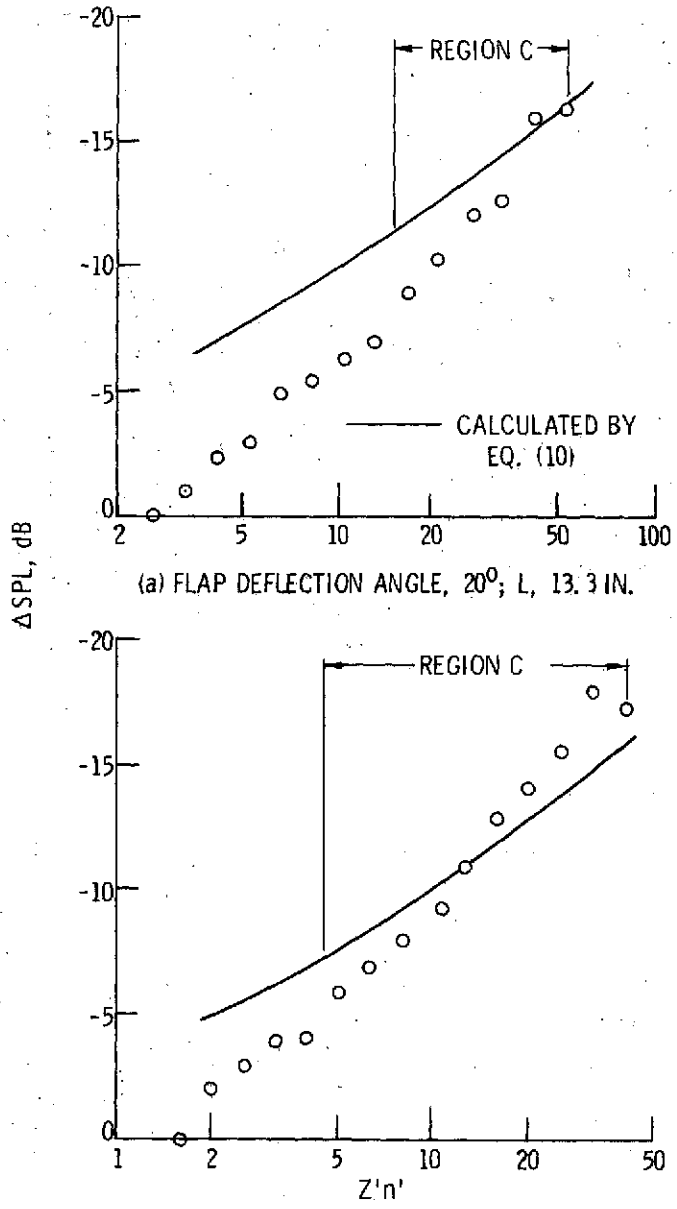

Figure 15. - Comparison of measured and calculated jet noise shielding benefits using 8-lobed mixer nozzle and two flap deflection angles. U_j, 744 ft/sec; directivity angle, 100°.

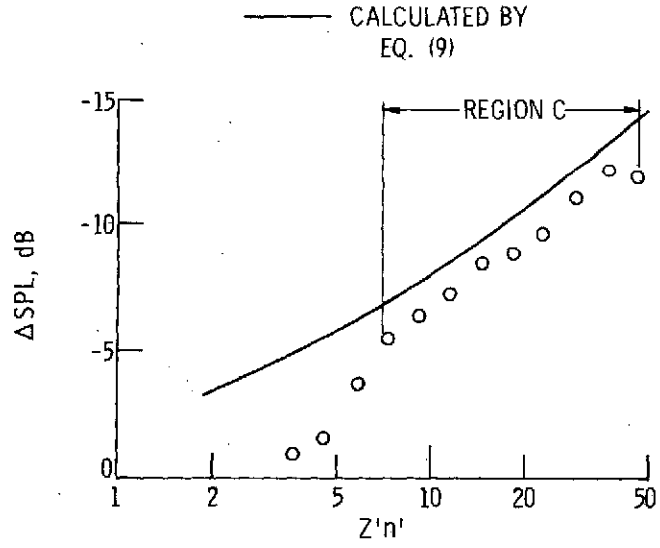

Figure 16. - Comparison of measured and calculated jet noise shielding benefits using 7-lobed mixer nozzle. U_j, 670 ft/sec; directivity angle, 90^0; L, 75 in.

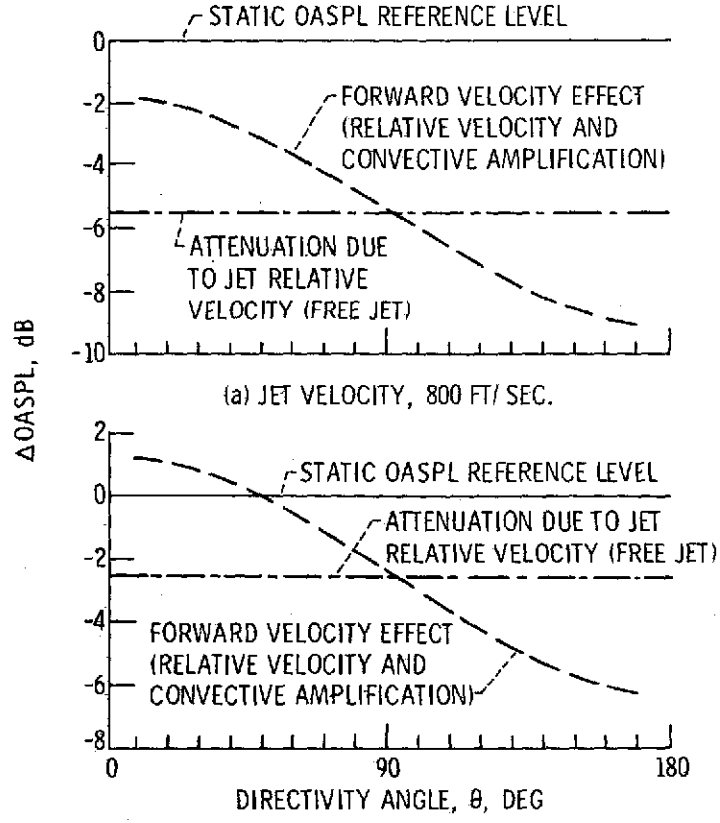

Figure 17. - Illustration of expected effect of forward velocity on OASPL of CTOL-OTW configuration. U_o, 150 ft/sec; a_o, 1120 ft/sec.

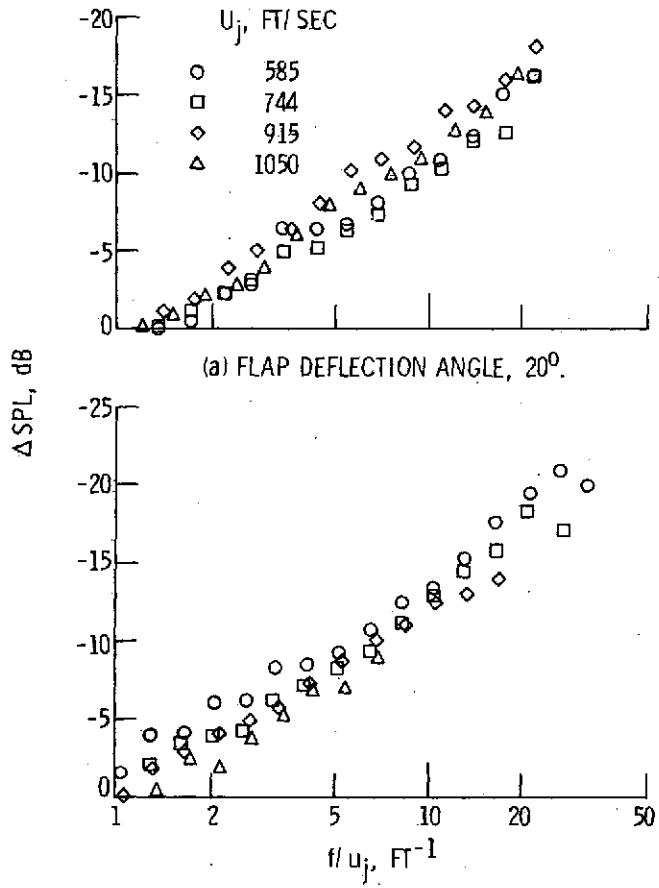

(a) FLAP DEFLECTION ANGLE, 20^0.

(b) FLAP DEFLECTION ANGLE, 60^0.

Figure 18. - Normalization of ΔSPL for 8-lobed orifice nozzle with wing for various jet velocities. Flaps deflected; directivity angle, θ, 100^0.

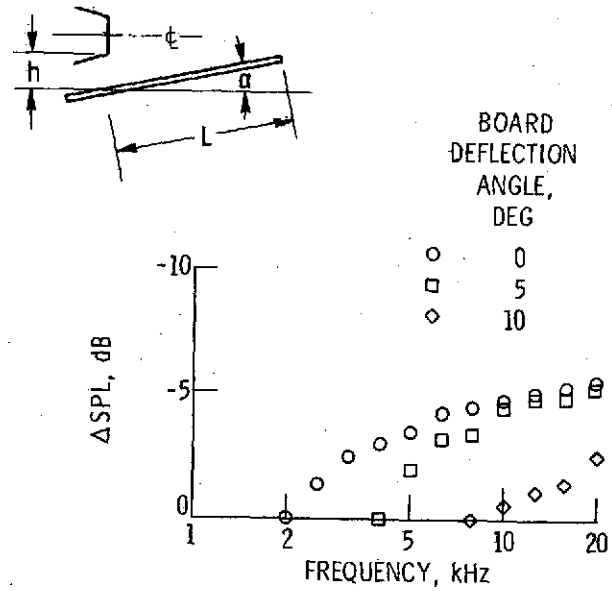

Figure 19. - Effect of jet-to-surface angle on shielding. Nozzle diam, 2.14-in.; surface length, L, 10.4-in.; h, 1.25-in.; jet velocity, 672 ft/sec; directivity angle, θ, 90^0.